

Contribution from the Department of Chemistry and Laboratory for Molecular Structure and Bonding, Texas A&M University, College Station, Texas 77843, and Department of Chemistry, Kalamazoo College, Kalamazoo, Michigan 49007

## Tetrahalobis(diphosphine)dimolybdenum(II) Compounds: $\beta$ Isomers with Seven-Membered Rings

F. Albert Cotton,\*<sup>1a</sup> Larry R. Falvello,<sup>1a</sup> Dawn R. Root,<sup>1b</sup> Thomas J. Smith,\*<sup>1b</sup> and K. Vidyasagar<sup>1a</sup>

Received September 25, 1989

The compound  $\beta$ -Mo<sub>2</sub>Cl<sub>4</sub>(1,3-dppp)<sub>2</sub>, where 1,3-dppp represents Ph<sub>2</sub>PCH<sub>2</sub>CH<sub>2</sub>CH<sub>2</sub>PPh<sub>2</sub>, has now been obtained in crystalline form, and its structure has been determined. The  $\beta$ -Mo<sub>2</sub>Br<sub>4</sub>(1,3-dppp)<sub>2</sub> analogue has also been prepared. The presence of seven-membered MoMoPCCCP rings has been confirmed and the ring conformation established in detail.  $\beta$ -Mo<sub>2</sub>Cl<sub>4</sub>(1,3-dppp)<sub>2</sub> crystallizes in space group *P*1 with *Z* = 4. The unit cell dimensions are *a* = 16.150 (4) Å, *b* = 19.054 (5) Å, *c* = 19.622 (5) Å,  $\alpha$  = 72.67 (2)°,  $\beta$  = 87.06 (2)°,  $\gamma$  = 87.46 (2)°, and *V* = 5754 (3) Å<sup>3</sup>. Each of the two crystallographically independent molecular sites is occupied by a principal isomer and a secondary isomer with P:S ratios of 3:1 and 2:1. As in all previous cases, at each site only one set of ligand atoms could be located and refined, but the two differently oriented (essentially perpendicular) Mo<sub>2</sub> units were easily recognized. The two P and two S isomers form very similar pairs, but P and S isomers have opposite chiralities. Average P-Mo-Mo-P twist angles for P and S isomers are -70.3 [2] and 74 [2]°, respectively, at one molecular site (site A) and are 68.5 [6] and -74.7 [4]°, respectively, at the other (site B). Mo-Mo, Mo-Cl, and Mo-P distances are perhaps slightly different in the P and S isomers.

### Introduction

Several years ago, in a study<sup>2</sup> of the formation of Mo<sub>2</sub>Cl<sub>4</sub>(Ph<sub>2</sub>P(CH<sub>2</sub>)<sub>n</sub>PPh<sub>2</sub>)<sub>2</sub> (*n* = 1-3) complexes in alcohol solvents, two compounds of formula Mo<sub>2</sub>Cl<sub>4</sub>(1,3-dppp)<sub>2</sub>, where 1,3-dppp is 1,3-bis(diphenylphosphino)propane, were obtained. On the basis of physical measurements, a chelating diphosphine structure was proposed for one isomer ( $\alpha$  isomer) while a bridging diphosphine ligand was assigned to the other ( $\beta$ ) form. The nearly identical infrared spectra (4000-600 cm<sup>-1</sup>) for the  $\alpha$  complex and for Re<sub>2</sub>Cl<sub>4</sub>(1,3-dppp)<sub>2</sub>, whose chelating structure had been established by X-ray crystallography,<sup>3</sup> supported this structural proposal. The  $\alpha$  isomer was isolated rapidly from methanol reactions, whereas the  $\beta$  complex formed more slowly in 1-propanol. These results implied kinetic rather than thermodynamic reaction control in the preparation of the  $\alpha$  compound, a conclusion confirmed by the conversion of the  $\alpha$  to the  $\beta$  isomer upon extended reflux in methanol or 1-propanol.

The fact that  $\beta$ -Mo<sub>2</sub>Cl<sub>4</sub>(1,3-dppp)<sub>2</sub> is more stable than the  $\alpha$  form was a little bit surprising since it has seven-membered rings, whereas the  $\alpha$  form has six-membered rings and a fully eclipsed Mo-Mo bond. An effort was therefore made to see if  $\beta$ -Mo<sub>2</sub>Cl<sub>4</sub>(1,3-dppp)<sub>2</sub> could be obtained in crystalline form so that the stability and other properties such as its lower energy  $\delta \rightarrow \delta^*$  transition could be accounted for in detail. The preparation of the bromo analogue was also undertaken. Both of these studies are reported here.

### Experimental Section

**Starting Materials and Reaction Conditions.** (NH<sub>4</sub>)<sub>5</sub>[Mo<sub>2</sub>Cl<sub>8</sub>]Cl·H<sub>2</sub>O<sup>4</sup> and (NH<sub>4</sub>)<sub>4</sub>Mo<sub>2</sub>Br<sub>8</sub><sup>5</sup> were prepared by established methods. 1,3-Bis(diphenylphosphino)propane (1,3-dppp) was obtained from Strem Chemical Co. and used as received. All solvents were reagent grade and were deoxygenated by bubbling nitrogen gas through them for 15-30 min prior to use. All reflux reactions were carried out under a nitrogen atmosphere, and wooden boiling sticks were used to facilitate reflux and crystal growth. Microanalyses were performed by Galbraith Laboratories, Knoxville, TN.

**$\beta$ -Mo<sub>2</sub>Cl<sub>4</sub>(1,3-dppp)<sub>2</sub> Crystals.** This material was prepared in 1-propanol as described previously except that (NH<sub>4</sub>)<sub>5</sub>[Mo<sub>2</sub>Cl<sub>8</sub>]Cl·H<sub>2</sub>O was used in place of the less soluble K<sub>4</sub>Mo<sub>2</sub>Cl<sub>8</sub>.<sup>2</sup> A small portion of the product was dissolved in dichloromethane, the solution was filtered, and its volume was reduced by 50% by vacuum pumping. An equal volume of 1-propanol and half of this volume of diethyl ether were added, and

the solution was cooled to 0 °C. A few seed crystals from the original product were introduced, and after 2 days in a freezer, dark green crystals were recovered. Alternatively, the reaction of (NH<sub>4</sub>)<sub>5</sub>[Mo<sub>2</sub>Cl<sub>8</sub>]Cl·H<sub>2</sub>O (0.10 g, 0.16 mmol) and 1,3-dppp (0.13 g, 0.32 mmol) in acetone (10 mL) yielded a deep green solution and unreacted Mo<sub>2</sub>Cl<sub>8</sub><sup>4-</sup> after a 24-h reflux. The latter was removed by filtration, and the filtrate was kept at 0 °C for 3 days, during which time a small quantity of dark green crystals was produced.

**$\beta$ -Mo<sub>2</sub>Br<sub>4</sub>(1,3-dppp)<sub>2</sub>.** (NH<sub>4</sub>)<sub>4</sub>Mo<sub>2</sub>Br<sub>8</sub> (0.10 g, 0.11 mmol) and 1,3-dppp (0.10 g, 0.24 mmol) were refluxed in 1-propanol (20 mL). Within 5 min, a brown suspension had formed, and reflux was continued for 22 h. The reaction mixture was cooled and then filtered, and the product was washed with ethanol and diethyl ether and then vacuum-dried to give a brick red powder. Yield: 0.10 g, 63%. Anal. Calcd for C<sub>27</sub>H<sub>26</sub>Br<sub>2</sub>Mo<sub>2</sub>[MoBr<sub>2</sub>(1,3-dppp)]: C, 48.53; H, 3.93; Br, 23.91; Mo, 14.36. Found: C, 48.46; H, 4.18; Br, 23.51; Mo, 14.00. Infrared spectral data (solid state): 273 s, 260 sh m, 252 sh m cm<sup>-1</sup>. Electronic spectral data (solid state): 724 nm s, 565 vw, 502 s, 450 sh m, 388 vs. Electronic spectral data (CH<sub>2</sub>Cl<sub>2</sub> solution): 718 nm ( $\epsilon$  1870 M<sup>-1</sup> cm<sup>-1</sup>), 615 sh (80), 497 (950), 448 sh (300), 388 (4490). Similar reflux reactions in methanol or ethanol produced the same material in comparable yields. With shorter reaction times in the latter media, traces of blue or green contaminants were evident. Reaction in acetone yielded small brown crystals that were found to be unsuitable for X-ray diffraction.

**Physical Measurements.** Infrared spectra from 4000 to 200 cm<sup>-1</sup> were recorded as mineral oil mulls on a Pye Unicam SP3-300 spectrophotometer. Electronic absorption spectra were obtained with mulls and with CH<sub>2</sub>Cl<sub>2</sub> solutions on a Perkin-Elmer Model 559 UV/vis spectrophotometer or a Model 330 UV/vis/near-IR spectrophotometer.

**X-ray Crystallography.** A green crystal of  $\beta$ -Mo<sub>2</sub>Cl<sub>4</sub>(1,3-dppp)<sub>2</sub> was mounted on a glass fiber and covered with a thin layer of epoxy cement. Geometric and intensity data were gathered by an automated four-circle diffractometer (Nicolet P3/F equivalent), using procedures described previously.<sup>6</sup> The reduced cell was found to be triclinic; however, the Niggli matrix suggested a possible transformation to a centered monoclinic cell. We were able to rule out this transformation for two reasons. First, in a careful determination of the cell parameters (the results are listed in Table I), we found that the cell dimensions differed by small but significant amounts from values that would lead to a valid transformation. Second, we used normal-beam oscillation photography to verify the lengths of lattice vectors and the absence of mirror symmetry in the diffraction pattern. Photos were made for all of the cell edges, as well as all of the face and body diagonals. Either of the lattice vectors [011] and [01 $\bar{1}$ ] would become a symmetry axis in one of two monoclinic transformations, but photos of both of these axes clearly showed the absence of mirror symmetry.

The  $\omega$ -2 $\theta$  scan technique was used to scan data points over one hemisphere of reciprocal space. Three monitor reflections were measured periodically during data collection; these did not show a significant change in intensity during 213.4 h of X-ray exposure. The data were reduced by standard algorithms.<sup>7</sup> An empirical absorption correction

(1) (a) Texas A&M University. (b) Kalamazoo College.  
 (2) Cole, N. F.; Derringer, D. R.; Fiore, E. A.; Knoechel, D. J.; Schmitt, R. K.; Smith, T. J. *Inorg. Chem.* **1985**, *24*, 1978.  
 (3) Cole, N. F.; Cotton, F. A.; Powell, G. L.; Smith, T. J. *Inorg. Chem.* **1983**, *22*, 2618.  
 (4) Brencic, J.; Cotton, F. A. *Inorg. Chem.* **1970**, *9*, 346.  
 (5) Brencic, J.; Leban, I.; Segedin, P. Z. *Anorg. Allg. Chem.* **1976**, *427*, 85.

(6) Cotton, F. A.; Frenz, B. A.; Deganello, G.; Shaver, A. J. *Organomet. Chem.* **1973**, *50*, 227.

Table I. Crystal Data for  $\beta$ -Mo<sub>2</sub>Cl<sub>4</sub>(dppp)<sub>2</sub>·1.5Me<sub>2</sub>CO

formula	Mo <sub>2</sub> Cl <sub>4</sub> P <sub>4</sub> C <sub>54</sub> H <sub>52</sub> · 1.5C <sub>3</sub> H <sub>6</sub> O
<i>a</i> , Å	16.150 (4)
<i>b</i> , Å	19.054 (5)
<i>c</i> , Å	19.622 (5)
$\alpha$ , deg	72.67 (2)
$\beta$ , deg	87.06 (2)
$\gamma$ , deg	87.46 (2)
<i>V</i> , Å <sup>3</sup>	5754 (3)
<i>Z</i>	4
fw	1245.73
space group	<i>P</i> $\bar{1}$
temp, °C	21 ± 1
radiation monochromated in incident beam ( $\lambda$ , Å)	Mo K $\alpha$ , 0.71073
<i>d</i> <sub>calc</sub> , g/cm <sup>3</sup>	1.438
$\mu$ (Mo K $\alpha$ ), cm <sup>-1</sup>	7.607
transm factors, %:	99.99, 82.18
max, min	
<i>R</i> <sup>a</sup>	0.0781
<i>R</i> <sub>w</sub> <sup>b</sup>	0.0787

$$^a R = \frac{\sum ||F_o| - |F_c||}{\sum |F_o|}; \quad ^b R_w = \frac{[\sum w(|F_o| - |F_c|)^2 / \sum w|F_o|^2]^{1/2}}{1 / [\sigma^2(|F_o|) + 0.001(|F_o|)^2]}$$

was applied,<sup>8</sup> based on azimuthal scans of eight reflections with setting angles ( $\chi$ ) near 90°.

The structure was solved by direct methods (SHELXS-86), which revealed over 100 of the 144 unique atomic sites in the asymmetric unit. The remaining atoms were located in difference Fourier maps following least-squares refinement.

To facilitate the explanation of the refinement, a preliminary description of the structure is needed. The crystallographic asymmetric unit comprises two independent molecular sites, which we have called the A and B sites. At each molecular site, a single set of ligand atoms is shared by two distinct pairs of Mo atoms, in the type of disorder that is now well-known to occur in most compounds of this kind. The two metal-metal bonds at a given molecular site have a common midpoint and are essentially perpendicular to each other. Thus, there are four molecules to consider—principal (P) and secondary (S) molecules at each of two sites. The principal molecules at the A and B sites are very similar but are conformational enantiomers at the chromophore; they differ significantly in nonsystematic ways at the periphery of the ligands. The secondary molecules at the A and B sites are also conformational enantiomers at their chromophores. In addition, the principal and secondary molecule at each site have opposite twists about their metal-metal bonds.

In all, there are 144 unique atomic sites in the crystallographic asymmetric unit. In the early and middle stages of refinement, all atoms were refined freely in each cycle. At each molecular site, the populations of the principal and secondary molybdenum pairs were refined, subject to the constraint that the total Mo<sub>2</sub> population at a given molecular site be 1.0. The populations converged to give P:S population ratios of 3:1 for the A site and 2:1 for the B site. The populations were both significant and determinate. We tried different starting values for the populations, always with the same results. Also, we observed that fixing the populations at values different from those resulting from the refinement led to significantly worse least-squares residuals.

Because of the large number of variable parameters involved, we conducted the final refinement in blocks. The final refinement sequence was as follows: First, all of the parameters for molecules at the A site were refined. Next, all parameters for the molecules at the B site were refined. Then, the parameters for three interstitial acetone molecules were refined in a cycle which also included the Mo, Cl, P, and propylene carbon atoms for site A; then the acetone parameters were refined along with the core parameters for site B. Finally, we repeated the individual cycles for site A and site B. The atoms of the acetone molecules were treated with isotropic displacement parameters; all other atomic sites were anisotropic. All phenyl groups were refined as rigid groups after idealization to regular hexagons. Although 1047 variable parameters were used for the model, the maximum number refined in any cycle was 499, corresponding to a data-to-parameter ratio of 11.7. The refinement converged with the residuals given in Table I.

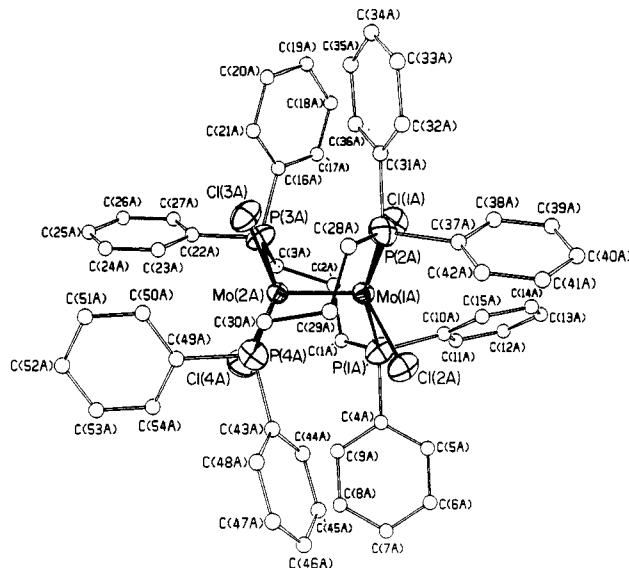


Figure 1. ORTEP drawing of the major (P) component of  $\beta$ -Mo<sub>2</sub>Cl<sub>4</sub>(1,3-dppp)<sub>2</sub> at the molecule A site. Carbon atoms are represented as circles of arbitrary radius. Mo, Cl, and P atoms are shown as their 50% probability ellipsoids.

## Results and Discussion

**Preparations.** As previously reported, the  $\alpha$  isomer of Mo<sub>2</sub>Cl<sub>4</sub>(1,3-dppp)<sub>2</sub> can be isolated as a pure compound and its thermal transformation to the  $\beta$  isomer can be followed in a higher boiling solvent such as 1-propanol. On the other hand, no way has yet been found to isolate  $\alpha$ -Mo<sub>2</sub>Br<sub>4</sub>(1,3-dppp)<sub>2</sub>. Reflux reactions in methanol, ethanol, and 1-propanol employing (N-H<sub>4</sub>)<sub>4</sub>Mo<sub>2</sub>Br<sub>8</sub> all produced exclusively the  $\beta$  isomer, although small amounts of contaminants of other colors, possibly indicative of some  $\alpha$  isomer, are observed. Previously, the marginally greater stability of  $\alpha$ -Mo<sub>2</sub>Cl<sub>4</sub>(dppe)<sub>2</sub> (dppe = Ph<sub>2</sub>PCH<sub>2</sub>CH<sub>2</sub>PPh<sub>2</sub>) over its bromo counterpart with respect to the  $\alpha \rightarrow \beta$  conversion has been noted.<sup>9,10</sup>

The spectroscopic properties of  $\beta$ -Mo<sub>2</sub>Br<sub>4</sub>(1,3-dppp)<sub>2</sub> resemble those of the Cl analogue reasonably closely. The infrared spectra above 600 cm<sup>-1</sup> for these compounds are very similar, while below this range a band at 273 cm<sup>-1</sup> in the former compound is assigned to  $\nu$ (Mo-Br); the ratio of this value to  $\nu$ (Mo-Cl)<sup>2</sup> at 335 cm<sup>-1</sup> is 0.81, which is acceptable for M-X stretching vibrations. In the electronic absorption spectra there is good qualitative correspondence between the  $\beta$ -Mo<sub>2</sub>X<sub>4</sub>(1,3-dppp)<sub>2</sub> materials. All bands undergo a red shift upon substitution of Br for Cl. This may account for the color differences between these species (Cl, green; Br, brown) although different rotational twist angles may also occur and shift the  $\delta \rightarrow \delta^*$  bands.

**Crystal Structure.** The results of the structure determination are compactly summarized by the positional parameters listed in Table II. As already mentioned in describing the method of refinement, there are entire, independent molecular sites at two different positions, A and B. Moreover, at each site there are two approximately perpendicular pairs of metal atoms, i.e., Mo(1A)-Mo(2A) together with Mo(3A)-Mo(4A) at site A and Mo(1B)-Mo(2B) together with Mo(3B)-Mo(4B) at site B. The Mo(1)-Mo(2) and Mo(3)-Mo(4) pairs are assumed to belong to different molecules which, however, occupy the site (in different unit cells) in such a way that the sets of ligand atoms are so similarly placed that they are indistinguishable. Thus, at each site, we refine one set of ligand atoms but two pairs of metal atoms. The two pairs are not equally populated. At the A sites the Mo(1)-Mo(2) pair is found 75% of the time and the Mo(3)-Mo(4) pair 25% of the time. We say that at site A we have a

(7) Calculations were done on a Local Area VAX cluster (VMS V4.6), with the programs SHELXS-86, SHELX-76, and the commercial package SDP/V V3.0.

(8) North, A. C. T.; Phillips, D. C.; Mathews, F. S. *Acta Crystallogr., Sect. A: Cryst. Phys., Diff., Theor. Gen. Crystallogr.* **1968**, *24*, 351.

(9) Agaskar, P. A.; Cotton, F. A.; Derringer, D. R.; Powell, G. L.; Root, D. R.; Smith, T. J. *Inorg. Chem.* **1985**, *24*, 2786.

(10) Fraser, I. F.; McVitie, A.; Peacock, R. D. *J. Chem. Res.* **1984**, 420.

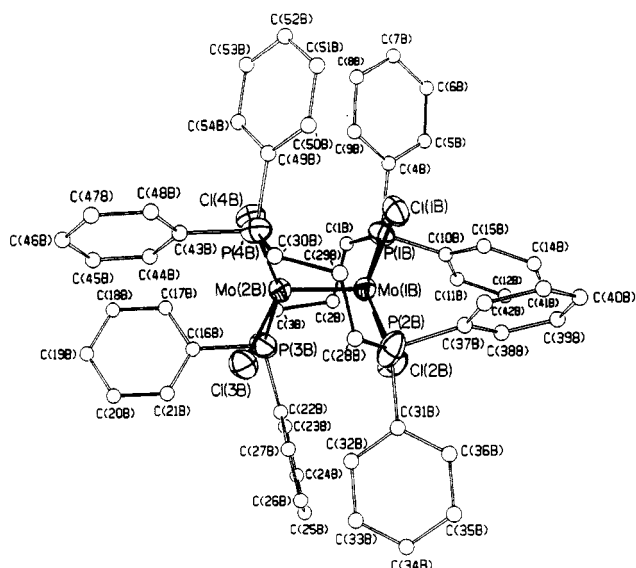


**Figure 2.** ORTEP drawing of the major (P) component of  $\beta$ - $\text{Mo}_2\text{Cl}_4(1,3\text{-dppp})_2$  at the molecule B site. Carbon atoms are represented as circles of arbitrary radius. The Mo, Cl, and P atoms are shown by their 50% probability ellipsoids.

ratio of principal to secondary molecules, a P:S ratio, of 3. At the B sites the P:S ratio is 2.

The sets of ligand atoms at both A and B sites have essentially identical spatial arrangements. Each set has only one symmetry element, a 2-fold axis that coincides with the Mo-Mo axis in the principal molecule at that site. Thus, each ligand arrangement is chiral. Those at the two A sites have opposite chirality (opposite helicity), and the same can be said for those at the two B sites.

Figures 1 and 2 show the principal molecules,  $\text{P}_A$  and  $\text{P}_B$ , at sites A and B, respectively. From these drawings, the overall structure is evident.  $\text{P}_A$  and  $\text{P}_B$  have essentially identical structures, although small but real differences occur around the periphery. The conformations of the 7-membered rings are such that the molecules have a  $C_2$  axis coinciding with the Mo-Mo bonds, as already noted. The drawings in Figures 1 and 2 show a  $\text{P}_A$  molecule of one chirality ( $\Delta$ ) and a  $\text{P}_B$  molecule of the opposite chirality ( $\Lambda$ ). The same thing can be seen in the end-on views presented in Figure 3a for the same  $\text{P}_A$  molecule ( $\text{P}_A^A$ ) and in Figure 3b for the same  $\text{P}_B$  molecule ( $\text{P}_B^A$ ).

The secondary molecules,  $\text{S}_A$  and  $\text{S}_B$ , at each site have different structures from the  $\text{P}_A$  and  $\text{P}_B$  molecules. For these S molecules the  $C_2$  axis of the ligand configuration lies perpendicular to the Mo-Mo axis and the ring conformations are, accordingly, related to each other in a different way. Comparison of parts a and b of Figure 3 and, again, of parts a and b of Figure 4 should make this clear. As with the P molecules, the S molecules have opposite chiralities at each of the two members of each pair of sites. That is, at the A sites there is one  $\text{S}_A^A$  and one  $\text{S}_A^B$  molecule and at the B sites one  $\text{S}_B^A$  and one  $\text{S}_B^B$  molecule. Overall, the crystalline solid is racemic in S molecules as well as in P molecules.

As is now well-known for all previous examples of this type of disorder, at a given position the P and S molecules have opposite directions of twist about the M-M bonds. If at a given A site there are  $\text{P}_A^A$  molecules in some cells, there will be  $\text{S}_A^A$  molecules in the others.

Selected bond distances and angles are presented in Table III. **Molecular Structure.** The Mo-Mo distances in the four crystallographically independent molecules range from 2.128 (12) Å in  $\text{S}_A$  to 2.156 (3) Å in  $\text{P}_A$ . For the molecules at B sites, we have 2.144 (4) Å for  $\text{P}_B$  and 2.134 (7) Å for  $\text{S}_B$ . None of these differences is statistically significant at the  $3\sigma$  level; even between the largest and smallest values the difference is 0.028 (12) Å. The pattern does suggest, however, that the distances in the S molecules are either slightly shorter than those in the P isomers or systematically underestimated. They could be genuinely shorter, since P and S molecules are truly different isomers.

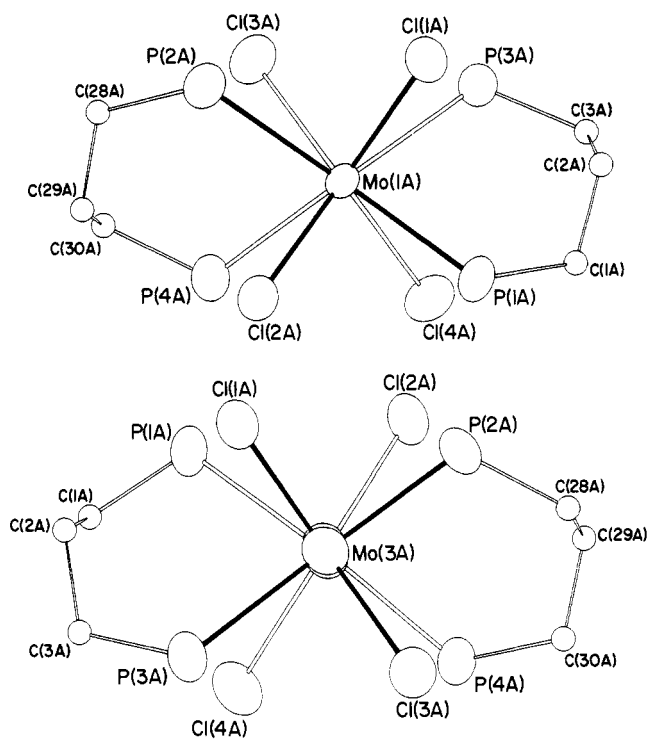


**Figure 3.** ORTEP drawings of the molecular cores of the (a, top) major (P) and (b, bottom) minor (S) components at the molecule A site: (a) atom Mo(2A) obscured by Mo(1A); (b) atom Mo(4A) obscured by Mo(3A).

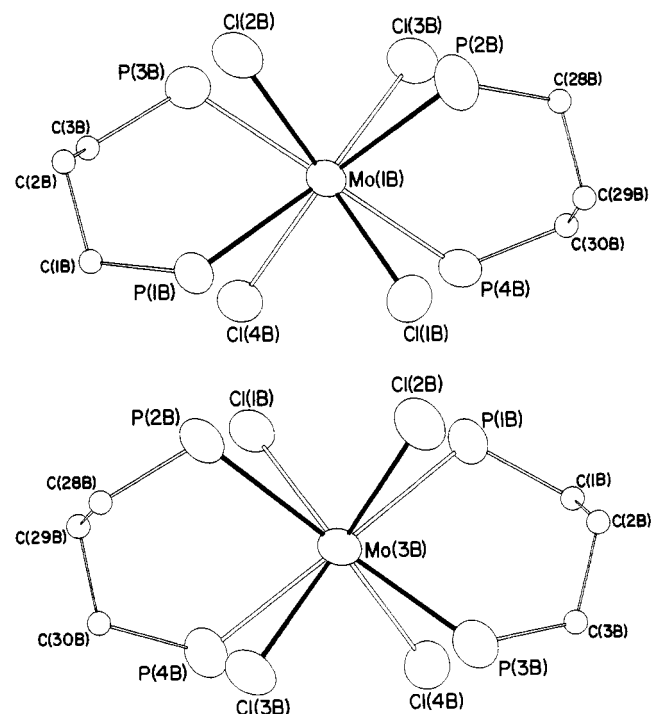


**Figure 4.** ORTEP drawings of the molecular cores of the (a) major (P) and (b) minor (S) components at the molecule B site: (a) atom Mo(2B) obscured by Mo(1B); (b) atom Mo(4B) obscured by Mo(3B).

When one compares the many crystallographically independent values of the Mo-Cl and Mo-P distances for the four independent molecules  $\text{P}_A$ ,  $\text{P}_B$ ,  $\text{S}_A$ , and  $\text{S}_B$ , the effects of disorder on the precision of the structure are of great importance. Since the observed and refined set of ligand atoms is the unresolved superposition of the ones that would be correct for the P and S molecules, it cannot be exactly the correct one for either molecule. It should be more nearly correct for the P molecule, and the more dominant the P molecule is, the more nearly correct should the

Table II. Positional Parameters and Their Estimated Standard Deviations for  $\beta$ -Mo<sub>2</sub>Cl<sub>4</sub>(dppp)<sub>2</sub>·1.5Me<sub>2</sub>CO

atom	x	y	z	B, <sup>a</sup> Å <sup>2</sup>	atom	x	y	z	B, <sup>a</sup> Å <sup>2</sup>
Mo(1A) <sup>b</sup>	0.8560 (1)	0.2754 (1)	0.4483 (1)	2.36 (6)	Cl(3B)	0.6221 (4)	0.6371 (3)	0.2281 (3)	4.5 (2)
Mo(2A) <sup>b</sup>	0.8766 (1)	0.2301 (1)	0.3602 (1)	2.25 (6)	Cl(4B)	0.6364 (3)	0.8851 (3)	0.1294 (3)	4.1 (2)
Mo(3A) <sup>c</sup>	0.8174 (5)	0.2163 (4)	0.4254 (4)	4.5 (2)	P(1B)	0.6205 (3)	0.8724 (3)	-0.0448 (3)	3.5 (1)
Mo(4A) <sup>c</sup>	0.9183 (6)	0.2877 (4)	0.3881 (5)	5.1 (3)	P(2B)	0.7038 (4)	0.6063 (3)	0.0613 (3)	4.6 (2)
Cl(1A)	0.7108 (3)	0.2820 (3)	0.4775 (3)	4.0 (1)	P(3B)	0.4749 (4)	0.7745 (3)	0.1424 (3)	4.0 (2)
Cl(2A)	0.9813 (3)	0.3036 (3)	0.4937 (3)	4.0 (1)	P(4B)	0.7831 (4)	0.7423 (3)	0.1838 (3)	3.8 (2)
Cl(3A)	0.8485 (4)	0.1004 (3)	0.4029 (3)	4.6 (2)	C(1B)	0.527 (1)	0.927 (1)	-0.027 (1)	4.2 (6)
Cl(4A)	0.9190 (4)	0.3207 (3)	0.2514 (3)	4.8 (2)	C(2B)	0.445 (1)	0.879 (1)	0.004 (1)	4.4 (6)
P(1A)	0.8432 (4)	0.4138 (3)	0.3813 (3)	3.8 (2)	C(3B)	0.439 (1)	0.866 (1)	0.088 (1)	3.4 (6)
P(2A)	0.8644 (4)	0.1548 (3)	0.5534 (3)	3.8 (2)	C(4B)	0.6930 (8)	0.9470 (6)	-0.0772 (7)	3.3 (6)
P(3A)	0.7323 (4)	0.2522 (3)	0.3049 (3)	3.8 (2)	C(5B)	0.6918 (8)	0.9941 (6)	-0.1469 (7)	4.9 (7)
P(4A)	1.0296 (4)	0.1888 (3)	0.3715 (3)	3.8 (2)	C(6B)	0.7448 (8)	1.0533 (6)	-0.1683 (7)	5.6 (8)
C(1A)	0.782 (1)	0.444 (1)	0.301 (1)	4.0 (6)	C(7B)	0.7990 (8)	1.0653 (6)	-0.1201 (7)	6.7 (9)
C(2A)	0.699 (1)	0.405 (1)	0.307 (1)	3.6 (6)	C(8B)	0.8002 (8)	1.0181 (6)	-0.0504 (7)	5.9 (8)
C(3A)	0.699 (1)	0.348 (1)	0.260 (1)	4.2 (6)	C(9B)	0.7472 (8)	0.9590 (6)	-0.0290 (7)	4.6 (7)
C(4A)	0.9311 (7)	0.4748 (7)	0.3506 (9)	3.3 (6)	C(10B)	0.602 (1)	0.8511 (8)	-0.1271 (6)	3.9 (6)
C(5A)	0.9588 (7)	0.5123 (7)	0.3959 (9)	6.7 (9)	C(11B)	0.525 (1)	0.8642 (8)	-0.1593 (6)	6.7 (9)
C(6A)	1.0242 (7)	0.5603 (7)	0.3734 (9)	8 (1)	C(12B)	0.513 (1)	0.8428 (8)	-0.2201 (6)	9 (1)
C(7A)	1.0619 (7)	0.5709 (7)	0.3057 (9)	8 (1)	C(13B)	0.578 (1)	0.8082 (8)	-0.2487 (6)	10 (1)
C(8A)	1.0342 (7)	0.5335 (7)	0.2604 (9)	6.8 (9)	C(14B)	0.655 (1)	0.7951 (8)	-0.2165 (6)	9 (1)
C(9A)	0.9688 (7)	0.4854 (7)	0.2828 (9)	4.8 (7)	C(15B)	0.666 (1)	0.8166 (6)	-0.1557 (6)	4.7 (7)
C(10A)	0.7853 (9)	0.4561 (9)	0.4451 (9)	4.3 (7)	C(16B)	0.4546 (9)	0.7807 (9)	0.2342 (6)	4.4 (7)
C(11A)	0.7406 (9)	0.5224 (9)	0.4196 (9)	9 (1)	C(17B)	0.4665 (9)	0.8465 (9)	0.2493 (6)	5.7 (8)
C(12A)	0.7019 (9)	0.5560 (9)	0.4675 (9)	12 (2)	C(18B)	0.4540 (9)	0.8503 (9)	0.3190 (6)	8 (1)
C(13A)	0.7079 (9)	0.5232 (9)	0.5409 (9)	13 (2)	C(19B)	0.4297 (9)	0.7883 (9)	0.3737 (6)	7 (1)
C(14A)	0.7526 (9)	0.4569 (9)	0.5664 (9)	11 (2)	C(20B)	0.4179 (9)	0.7224 (9)	0.3587 (6)	7 (1)
C(15A)	0.7913 (9)	0.4234 (9)	0.5185 (9)	7 (1)	C(21B)	0.4303 (9)	0.7186 (9)	0.2889 (6)	5.8 (7)
C(16A)	0.6360 (9)	0.2078 (9)	0.3517 (7)	5.0 (7)	C(22B)	0.393 (1)	0.712 (1)	0.1364 (9)	5.8 (8)
C(17A)	0.5725 (9)	0.2474 (9)	0.3760 (7)	5.7 (8)	C(23B)	0.314 (1)	0.739 (1)	0.1142 (9)	6.9 (9)
C(18A)	0.5042 (9)	0.2111 (9)	0.4149 (7)	7 (1)	C(24B)	0.253 (1)	0.691 (1)	0.1115 (9)	11 (1)
C(19A)	0.4993 (9)	0.1351 (9)	0.4295 (7)	8 (1)	C(25B)	0.271 (1)	0.615 (1)	0.1310 (9)	11 (2)
C(20A)	0.5628 (9)	0.0955 (9)	0.4051 (7)	6.9 (9)	C(26B)	0.350 (1)	0.588 (1)	0.1532 (9)	12 (1)
C(21A)	0.6311 (9)	0.1318 (9)	0.3662 (7)	5.2 (7)	C(27B)	0.411 (1)	0.637 (1)	0.1559 (9)	9 (1)
C(22A)	0.738 (1)	0.2195 (9)	0.2259 (8)	5.7 (8)	C(28B)	0.782 (1)	0.567 (1)	0.130 (1)	4.5 (6)
C(23A)	0.807 (1)	0.1755 (9)	0.2166 (8)	7.0 (9)	C(29B)	0.853 (1)	0.618 (1)	0.135 (1)	6.1 (8)
C(24A)	0.814 (1)	0.1496 (9)	0.1571 (8)	9 (1)	C(30B)	0.841 (1)	0.654 (1)	0.198 (1)	4.6 (7)
C(25A)	0.752 (1)	0.1676 (9)	0.1068 (8)	9 (1)	C(31B)	0.634 (1)	0.5283 (7)	0.0777 (8)	4.1 (6)
C(26A)	0.684 (1)	0.2116 (9)	0.1161 (8)	6.2 (9)	C(32B)	0.580 (1)	0.5106 (7)	0.1378 (8)	6.1 (8)
C(27A)	0.677 (1)	0.2375 (9)	0.1756 (8)	6.6 (9)	C(33B)	0.531 (1)	0.4491 (7)	0.1522 (8)	6.9 (9)
C(28A)	0.955 (1)	0.087 (1)	0.559 (1)	4.6 (6)	C(34B)	0.536 (1)	0.4052 (7)	0.1064 (8)	8 (1)
C(29A)	1.038 (1)	0.117 (1)	0.523 (1)	5.1 (7)	C(35B)	0.589 (1)	0.4229 (7)	0.0462 (8)	9 (1)
C(30A)	1.052 (1)	0.106 (1)	0.447 (1)	4.3 (6)	C(36B)	0.639 (1)	0.4844 (7)	0.0319 (8)	5.8 (8)
C(31A)	0.7800 (8)	0.0890 (7)	0.5860 (7)	3.7 (6)	C(37B)	0.760 (1)	0.6066 (9)	-0.0238 (8)	5.6 (8)
C(32A)	0.7928 (8)	0.0341 (7)	0.6501 (7)	4.4 (7)	C(38B)	0.716 (1)	0.6273 (9)	-0.0860 (8)	11 (1)
C(33A)	0.7354 (8)	-0.0213 (7)	0.6758 (7)	5.2 (7)	C(39B)	0.753 (1)	0.6233 (9)	-0.1504 (8)	12 (2)
C(34A)	0.6653 (8)	-0.0216 (7)	0.6372 (7)	5.9 (8)	C(40B)	0.836 (1)	0.5986 (9)	-0.1526 (8)	16 (2)
C(35A)	0.6525 (8)	0.0334 (7)	0.5731 (7)	6.8 (9)	C(41B)	0.880 (1)	0.5778 (9)	-0.0904 (8)	15 (2)
C(36A)	0.7099 (8)	0.0887 (7)	0.5475 (7)	5.7 (8)	C(42B)	0.843 (1)	0.5818 (9)	-0.0260 (8)	10 (1)
C(37A)	0.874 (1)	0.1860 (7)	0.6333 (6)	3.7 (6)	C(43B)	0.770 (1)	0.7451 (8)	0.2763 (6)	4.3 (7)
C(38A)	0.804 (1)	0.2210 (7)	0.6549 (6)	4.6 (7)	C(44B)	0.694 (1)	0.7640 (8)	0.3042 (6)	5.1 (8)
C(39A)	0.807 (1)	0.2469 (7)	0.7141 (6)	5.8 (8)	C(45B)	0.686 (1)	0.7628 (8)	0.3756 (6)	7.1 (9)
C(40A)	0.880 (1)	0.2378 (7)	0.7517 (6)	6.4 (9)	C(46B)	0.754 (1)	0.7427 (8)	0.4193 (6)	8 (1)
C(41A)	0.950 (1)	0.2029 (7)	0.7302 (6)	5.7 (8)	C(47B)	0.830 (1)	0.7238 (8)	0.3914 (6)	8 (1)
C(42A)	0.947 (1)	0.1770 (7)	0.6709 (6)	5.7 (8)	C(48B)	0.838 (1)	0.7250 (8)	0.3200 (6)	6.5 (9)
C(43A)	1.1179 (9)	0.245 (1)	0.3675 (9)	5.9 (9)	C(49B)	0.861 (1)	0.8126 (8)	0.1482 (8)	4.5 (7)
C(44A)	1.1044 (9)	0.321 (1)	0.3558 (9)	6.1 (8)	C(50B)	0.932 (1)	0.8006 (8)	0.1093 (8)	9 (1)
C(45A)	1.1712 (9)	0.366 (1)	0.3528 (9)	10 (1)	C(51B)	0.988 (1)	0.8570 (8)	0.0819 (8)	9 (1)
C(46A)	1.2515 (9)	0.335 (1)	0.3615 (9)	10 (1)	C(52B)	0.973 (1)	0.9252 (8)	0.0934 (8)	9 (1)
C(47A)	1.2651 (9)	0.260 (1)	0.3733 (9)	10 (1)	C(53B)	0.902 (1)	0.9372 (8)	0.1323 (8)	8 (1)
C(48A)	1.1983 (9)	0.215 (1)	0.3763 (9)	8 (1)	C(54B)	0.846 (1)	0.8809 (8)	0.1597 (8)	7.2 (9)
C(49A)	1.0493 (9)	0.1564 (9)	0.2916 (7)	4.4 (7)	C(1)	0.079 (3)	0.650 (3)	0.983 (3)	16 (1)*
C(50A)	1.0209 (9)	0.0884 (9)	0.2911 (7)	4.4 (7)	O(1)	0.066 (2)	0.642 (2)	1.050 (2)	20 (1)*
C(51A)	1.0355 (9)	0.0646 (9)	0.2307 (7)	7 (1)	C(2)	0.151 (3)	0.632 (2)	0.951 (2)	13 (1)*
C(52A)	1.0783 (9)	0.1087 (9)	0.1709 (7)	10 (1)	C(3)	0.028 (2)	0.720 (2)	0.946 (2)	12 (1)*
C(53A)	1.1067 (9)	0.1767 (9)	0.1714 (7)	8 (1)	C(4)	0.483 (2)	0.442 (2)	0.392 (2)	10.6 (9)*
C(54A)	1.0922 (9)	0.2005 (9)	0.2317 (7)	6.8 (9)	O(2)	0.454 (1)	0.402 (1)	0.360 (1)	10.9 (6)*
Mo(1B) <sup>d</sup>	0.6576 (2)	0.7421 (1)	0.0348 (1)	2.84 (7)	C(5)	0.479 (2)	0.591 (2)	0.540 (2)	12 (1)*
Mo(2B) <sup>d</sup>	0.6359 (2)	0.7546 (1)	0.1394 (1)	2.92 (7)	C(6)	0.509 (2)	0.481 (2)	0.643 (2)	12 (1)*
Mo(3B) <sup>e</sup>	0.5988 (3)	0.7031 (3)	0.1014 (3)	3.2 (1)	C(7)	0.315 (2)	0.045 (3)	0.662 (2)	16 (1)*
Mo(4B) <sup>e</sup>	0.6828 (3)	0.7915 (3)	0.0740 (3)	2.9 (1)	O(3)	0.357 (2)	0.058 (2)	0.608 (2)	23 (2)*
Cl(1B)	0.7977 (3)	0.7696 (3)	-0.0014 (3)	3.9 (1)	C(8)	0.348 (2)	0.015 (2)	0.733 (2)	14 (1)*
Cl(2B)	0.5274 (4)	0.7068 (3)	-0.0024 (3)	4.9 (2)	C(9)	0.226 (2)	0.053 (3)	0.666 (2)	19 (2)*

<sup>a</sup> Values marked with an asterisk denote atoms that were refined isotropically. Values for anisotropically refined atoms are given in the form of the equivalent isotropic displacement parameter defined as  $(4/3)[a^2\beta_{11} + b^2\beta_{22} + c^2\beta_{33} + ab(\cos\beta)\beta_{12} + ac(\cos\beta)\beta_{13} + bc(\cos\alpha)\beta_{23}]$ . <sup>b</sup> Site modeled as 0.75 Mo. <sup>c</sup> Site modeled as 0.25 Mo. <sup>d</sup> Site modeled as 0.67 Mo. <sup>e</sup> Site modeled as 0.33 Mo.

**Table III.** Selected Bond Distances (Å) and Angles (deg) for  $\beta$ - $\text{Mo}_2\text{Cl}_4(\text{dppp})_2 \cdot 1.5\text{Me}_2\text{CO}$ 

Bond Distances							
Mo(1A)–Mo(2A)	2.156 (3)	Mo(4A)–P(4A)	2.625 (11)	Mo(1B)–Mo(2B)	2.144 (4)	Mo(4B)–P(4B)	2.676 (8)
Mo(1A)–Cl(1A)	2.393 (5)	P(1A)–C(1A)	1.83 (2)	Mo(1B)–Cl(1B)	2.369 (6)	P(1B)–C(1B)	1.86 (2)
Mo(1A)–Cl(2A)	2.396 (6)	P(1A)–C(4A)	1.836 (13)	Mo(1B)–Cl(2B)	2.447 (7)	P(1B)–C(4B)	1.824 (13)
Mo(1A)–P(1A)	2.577 (5)	P(1A)–C(10A)	1.87 (2)	Mo(1B)–P(1B)	2.572 (5)	P(1B)–C(10B)	1.822 (15)
Mo(1A)–P(2A)	2.593 (5)	P(2A)–C(28A)	1.89 (2)	Mo(1B)–P(2B)	2.567 (6)	P(2B)–C(28B)	1.87 (2)
Mo(2A)–Cl(3A)	2.418 (5)	P(2A)–C(31A)	1.849 (14)	Mo(2B)–Cl(3B)	2.404 (5)	P(2B)–C(31B)	1.848 (15)
Mo(2A)–Cl(4A)	2.400 (5)	P(2A)–C(37A)	1.849 (15)	Mo(2B)–Cl(4B)	2.435 (6)	P(2B)–C(37B)	1.86 (2)
Mo(2A)–P(3A)	2.585 (6)	P(3A)–C(3A)	1.84 (2)	Mo(2B)–P(3B)	2.611 (6)	P(3B)–C(3B)	1.84 (2)
Mo(2A)–P(4A)	2.560 (6)	P(3A)–C(16A)	1.868 (15)	Mo(2B)–P(4B)	2.550 (6)	P(3B)–C(16B)	1.853 (14)
Mo(3A)–Mo(4A)	2.128 (12)	P(3A)–C(22A)	1.83 (2)	Mo(3B)–Mo(4B)	2.134 (7)	P(3B)–C(22B)	1.84 (2)
Mo(3A)–Cl(1A)	2.442 (10)	P(4A)–C(30A)	1.86 (2)	Mo(3B)–Cl(2B)	2.373 (8)	P(4B)–C(30B)	1.84 (2)
Mo(3A)–Cl(3A)	2.406 (10)	P(4A)–C(43A)	1.81 (2)	Mo(3B)–Cl(3B)	2.469 (7)	P(4B)–C(43B)	1.834 (15)
Mo(3A)–P(2A)	2.573 (9)	P(4A)–C(49A)	1.86 (2)	Mo(3B)–P(2B)	2.711 (9)	P(4B)–C(49B)	1.84 (2)
Mo(3A)–P(3A)	2.690 (10)	C(1A)–C(2A)	1.55 (3)	Mo(3B)–P(3B)	2.597 (8)	C(1B)–C(2B)	1.63 (3)
Mo(4A)–Cl(2A)	2.455 (11)	C(2A)–C(3A)	1.64 (3)	Mo(4B)–Cl(1B)	2.414 (7)	C(2B)–C(3B)	1.59 (3)
Mo(4A)–Cl(4A)	2.566 (10)	C(28A)–C(29A)	1.55 (3)	Mo(4B)–Cl(4B)	2.425 (8)	C(28B)–C(29B)	1.56 (3)
Mo(4A)–P(1A)	2.612 (10)	C(29A)–C(30A)	1.56 (3)	Mo(4B)–P(1B)	2.604 (7)	C(29B)–C(30B)	1.58 (4)

Bond Angles							
Mo(2A)–Mo(1A)–Cl(1A)	110.2 (2)	Mo(1A)–P(1A)–C(4A)	124.8 (5)	Mo(2B)–Mo(1B)–Cl(1B)	108.3 (2)	Mo(1B)–P(1B)–C(4B)	125.2 (5)
Mo(2A)–Mo(1A)–Cl(2A)	113.6 (2)	Mo(1A)–P(1A)–C(10A)	105.3 (5)	Mo(2B)–Mo(1B)–Cl(2B)	107.8 (2)	Mo(1B)–P(1B)–C(10B)	99.2 (5)
Mo(2A)–Mo(1A)–P(1A)	100.8 (2)	Mo(4A)–P(1A)–C(1A)	109.7 (8)	Mo(2B)–Mo(1B)–P(1B)	101.2 (2)	Mo(4B)–P(1B)–C(1B)	111.0 (6)
Mo(2A)–Mo(1A)–P(2A)	99.3 (2)	Mo(4A)–P(1A)–C(4A)	99.5 (5)	Mo(2B)–Mo(1B)–P(2B)	103.0 (2)	Mo(4B)–P(1B)–C(4B)	103.7 (5)
Cl(1A)–Mo(1A)–Cl(2A)	136.2 (2)	Mo(4A)–P(1A)–C(10A)	136.6 (6)	Cl(1B)–Mo(1B)–Cl(2B)	143.9 (2)	Mo(4B)–P(1B)–C(10B)	130.9 (5)
Cl(1A)–Mo(1A)–P(1A)	86.8 (2)	C(1A)–P(1A)–C(4A)	98.9 (8)	Cl(1B)–Mo(1B)–P(1B)	86.6 (2)	C(1B)–P(1B)–C(4B)	98.9 (8)
Cl(1A)–Mo(1A)–P(2A)	87.6 (2)	C(1A)–P(1A)–C(10A)	103.5 (9)	Cl(1B)–Mo(1B)–P(2B)	86.4 (2)	C(1B)–P(1B)–C(10B)	106.0 (9)
Cl(2A)–Mo(1A)–P(1A)	86.3 (2)	C(4A)–P(1A)–C(10A)	102.3 (8)	Cl(2B)–Mo(1B)–P(1B)	85.6 (2)	C(4B)–P(1B)–C(10B)	101.1 (7)
Cl(2A)–Mo(1A)–P(2A)	84.4 (2)	Mo(1A)–P(2A)–C(28A)	121.2 (6)	Cl(2B)–Mo(1B)–P(2B)	86.4 (2)	Mo(1B)–P(2B)–C(28B)	119.0 (8)
P(1A)–Mo(1A)–P(2A)	159.8 (2)	Mo(1A)–P(2A)–C(31A)	125.7 (5)	P(1B)–Mo(1B)–P(2B)	155.7 (2)	Mo(1B)–P(2B)–C(31B)	125.6 (5)
Mo(1A)–Mo(2A)–Cl(3A)	108.2 (2)	Mo(1A)–P(2A)–C(37A)	104.4 (4)	Mo(1B)–Mo(2B)–Cl(3B)	111.0 (2)	Mo(1B)–P(2B)–C(37B)	101.4 (5)
Mo(1A)–Mo(2A)–Cl(4A)	112.6 (2)	Mo(3A)–P(2A)–C(28A)	113.9 (7)	Mo(1B)–Mo(2B)–Cl(4B)	108.5 (2)	Mo(3B)–P(2B)–C(28B)	110.6 (8)
Mo(1A)–Mo(2A)–P(3A)	101.2 (2)	Mo(3A)–P(2A)–C(31A)	99.1 (5)	Mo(1B)–Mo(2B)–P(3B)	100.8 (2)	Mo(3B)–P(2B)–C(31B)	99.2 (6)
Mo(1A)–Mo(2A)–P(4A)	101.9 (2)	Mo(3A)–P(2A)–C(37A)	134.7 (5)	Mo(1B)–Mo(2B)–P(4B)	101.4 (2)	Mo(3B)–P(2B)–C(37B)	134.2 (6)
Cl(3A)–Mo(2A)–Cl(4A)	139.2 (2)	C(28A)–P(2A)–C(31A)	98.7 (8)	Cl(3B)–Mo(2B)–Cl(4B)	140.4 (2)	C(28B)–P(2B)–C(31B)	101.1 (8)
Cl(3A)–Mo(2A)–P(3A)	88.3 (2)	C(28A)–P(2A)–C(37A)	103.2 (9)	Cl(3B)–Mo(2B)–P(3B)	89.9 (2)	C(28B)–P(2B)–C(37B)	104 (1)
Cl(3A)–Mo(2A)–P(4A)	85.4 (2)	C(31A)–P(2A)–C(37A)	99.8 (7)	Cl(3B)–Mo(2B)–P(4B)	82.7 (2)	C(31B)–P(2B)–C(37B)	103.2 (9)
Cl(4A)–Mo(2A)–P(3A)	83.8 (2)	Mo(2A)–P(3A)–C(3A)	118.0 (7)	Cl(4B)–Mo(2B)–P(3B)	83.9 (2)	Mo(2B)–P(3B)–C(3B)	113.8 (6)
Cl(4A)–Mo(2A)–P(4A)	86.5 (2)	Mo(2A)–P(3A)–C(16A)	123.9 (5)	Cl(4B)–Mo(2B)–P(4B)	88.5 (2)	Mo(2B)–P(3B)–C(16B)	101.3 (5)
P(3A)–Mo(2A)–P(4A)	156.8 (2)	Mo(2A)–P(3A)–C(22A)	107.7 (7)	P(3B)–Mo(2B)–P(4B)	157.8 (2)	Mo(2B)–P(3B)–C(22B)	129.6 (6)
Mo(4A)–Mo(3A)–Cl(1A)	107.6 (5)	Mo(3A)–P(3A)–C(3A)	122.1 (8)	Mo(4B)–Mo(3B)–Cl(2B)	108.1 (3)	Mo(3B)–P(3B)–C(3B)	122.3 (7)
Mo(4A)–Mo(3A)–Cl(3A)	109.9 (5)	Mo(3A)–P(3A)–C(16A)	93.4 (5)	Mo(4B)–Mo(3B)–Cl(3B)	105.2 (3)	Mo(3B)–P(3B)–C(16B)	125.5 (5)
Mo(4A)–Mo(3A)–P(2A)	98.2 (4)	Mo(3A)–P(3A)–C(22A)	133.0 (6)	Mo(4B)–Mo(3B)–P(2B)	95.6 (3)	Mo(3B)–P(3B)–C(22B)	97.0 (7)
Mo(4A)–Mo(3A)–P(3A)	98.7 (4)	C(3A)–P(3A)–C(16A)	104.8 (8)	Mo(4B)–Mo(3B)–P(3B)	96.5 (3)	C(3B)–P(3B)–C(16B)	101.7 (9)
Cl(1A)–Mo(3A)–Cl(3A)	142.4 (4)	C(3A)–P(3A)–C(22A)	97.2 (8)	Cl(3B)–Mo(3B)–Cl(3B)	146.7 (3)	C(3B)–P(3B)–C(22B)	104.8 (8)
Cl(1A)–Mo(3A)–P(2A)	87.1 (3)	C(16A)–P(3A)–C(22A)	101.1 (9)	Cl(2B)–Mo(3B)–P(2B)	84.7 (3)	C(16B)–P(3B)–C(22B)	101.3 (8)
Cl(1A)–Mo(3A)–P(3A)	88.8 (3)	Mo(2A)–P(4A)–C(30A)	115.1 (6)	Cl(2B)–Mo(3B)–P(3B)	89.6 (3)	Mo(2B)–P(4B)–C(30B)	119.5 (8)
Cl(3A)–Mo(3A)–P(2A)	87.2 (3)	Mo(2A)–P(4A)–C(43A)	127.6 (6)	Cl(3B)–Mo(3B)–P(2B)	90.0 (2)	Mo(2B)–P(4B)–C(43B)	104.7 (6)
Cl(3A)–Mo(3A)–P(3A)	86.2 (3)	Mo(2A)–P(4A)–C(49A)	101.8 (5)	Cl(3B)–Mo(3B)–P(3B)	88.8 (2)	Mo(2B)–P(4B)–C(49B)	123.3 (5)
P(2A)–Mo(3A)–P(3A)	163.1 (4)	Mo(4A)–P(4A)–C(30A)	120.1 (7)	P(2B)–Mo(3B)–P(3B)	167.7 (3)	Mo(4B)–P(4B)–C(30B)	120.7 (8)
Mo(3A)–Mo(4A)–Cl(2A)	107.2 (4)	Mo(4A)–P(4A)–C(43A)	95.3 (7)	Mo(3B)–Mo(4B)–Cl(1B)	111.6 (3)	Mo(4B)–P(4B)–C(43B)	130.7 (6)
Mo(3A)–Mo(4A)–Cl(4A)	105.2 (5)	Mo(4A)–P(4A)–C(49A)	127.4 (6)	Mo(3B)–Mo(4B)–Cl(4B)	110.5 (3)	Mo(4B)–P(4B)–C(49B)	95.4 (5)
Mo(3A)–Mo(4A)–P(1A)	99.8 (4)	C(30A)–P(4A)–C(43A)	103.3 (9)	Mo(3B)–Mo(4B)–P(1B)	99.9 (3)	C(30B)–P(4B)–C(43B)	99.8 (9)
Mo(3A)–Mo(4A)–P(4A)	97.8 (4)	C(30A)–P(4A)–C(49A)	103.4 (9)	Mo(3B)–Mo(4B)–P(4B)	98.7 (2)	C(30B)–P(4B)–C(49B)	104.5 (8)
Cl(2A)–Mo(4A)–Cl(4A)	147.6 (4)	C(43A)–P(4A)–C(49A)	102.3 (8)	Cl(1B)–Mo(4B)–Cl(4B)	137.9 (3)	C(43B)–P(4B)–C(49B)	100.7 (8)
Cl(2A)–Mo(4A)–P(1A)	84.3 (4)	P(1A)–C(1A)–C(2A)	114 (1)	Cl(1B)–Mo(4B)–P(1B)	85.0 (2)	P(1B)–C(1B)–C(2B)	115 (1)
Cl(2A)–Mo(4A)–P(4A)	94.4 (3)	C(1A)–C(2A)–C(3A)	113 (2)	Cl(1B)–Mo(4B)–P(4B)	87.1 (2)	C(1B)–C(2B)–C(3B)	107 (2)
Cl(4A)–Mo(4A)–P(1A)	89.6 (3)	P(3A)–C(3A)–C(2A)	116 (1)	Cl(4B)–Mo(4B)–P(1B)	88.8 (2)	P(3B)–C(3B)–C(2B)	115 (1)
Cl(4A)–Mo(4A)–P(4A)	81.8 (3)	P(2A)–C(28A)–C(29A)	117 (1)	Cl(4B)–Mo(4B)–P(4B)	85.9 (3)	P(2B)–C(28B)–C(29B)	117 (1)
P(1A)–Mo(4A)–P(4A)	161.9 (4)	C(28A)–C(29A)–C(30A)	112 (2)	P(1B)–Mo(4B)–P(4B)	161.4 (3)	C(28B)–C(29B)–C(30B)	115 (2)
Mo(1A)–P(1A)–C(1A)	119.2 (7)	P(4A)–C(30A)–C(29A)	115 (2)	Mo(1B)–P(1B)–C(1B)	123.1 (6)	P(4B)–C(30B)–C(29B)	120 (1)

\* Numbers in parentheses are estimated standard deviations in the least significant digits.

values be for it while at the same time, the worse they should be for the S molecule. Thus the P<sub>A</sub> molecule may be the most accurately defined one of the four and S<sub>B</sub> the least.

In the present crystal structure, we see evidence that these factors are at work. In the P molecules the Mo–Cl distances (eight independent ones) have highest, lowest, and average values of 2.447, 2.369, and 2.408 Å, while the corresponding figures for the S molecules are 2.566, 2.373, and 2.444 Å. The ranges for P and S molecules, respectively, are 0.078 and 0.193 Å. The former range is perhaps not atypical for a set of eight "chemically" equivalent but "crystallographically" nonequivalent distances, but a range of 0.193 Å is certainly well out of the ordinary for a normal, ordered structure. Probably the only figure that merits confidence is the average value for the P molecules, viz., 2.408 Å. Whether there is a real increase to 2.444 Å, that is of about 0.04 Å, in the S molecules is impossible to say with any assurance. Similarly, for the Mo–P distances, the values in the P molecules

cover a range of only 0.061 Å and have a mean of 2.577 Å, whereas those in the S isomers cover a range of 0.138 Å and the average is 2.636 Å.

Let us turn now to the torsion angles. All of the individual values are listed in the supplementary material. We give below only average values of (a) the smallest angles, as, for example P(1A)–Mo(1A)–Mo(2A)–Cl(4A) (see Figure 3) in P<sub>A</sub> as well as (b) the P–Mo–Mo–P angles, where the P atoms belong to the same ligand. Since both A and Δ molecules of both types are present, signs are ignored.

P<sub>A</sub>: 18.6 and 70.3°  
 P<sub>B</sub>: 19.8 and 68.5°  
 S<sub>A</sub>: 18.7 and 74.0°  
 S<sub>B</sub>: 16.8 and 74.7°

Thus, even though the A and B sites are crystallographically distinct, corresponding twist angles, like the other important inner

molecular dimensions, are very similar for both P and both S molecules. It is also interesting to see how very similar the twist angles in the S molecules are to those in the P molecules, despite the fact that the relationship of ligands to Mo<sub>2</sub> groups is different. The observed energy of the  $\delta \rightarrow \delta^*$  transition is in accord with the  $\beta$  structure with a torsion angle of ca. 18°, according to the previously published correlation.<sup>11</sup>

**Ring Conformations.** Now that we have seen that P and S isomers show only small, if not negligible, differences in bond lengths and bond angles involving their Mo<sub>2</sub> units, we must turn to the question of how they differ. The key, qualitative difference between the P and S molecules is to be found in the conformations of their seven-membered rings. This is most easily seen by comparing parts a and b of Figure 3 and parts a and b of Figure 4. In the P molecules, the two rings are interchanged by a 2-fold rotation about an *axis that coincides with the Mo–Mo bond*, whereas in the S molecules the rotation is about an *axis perpendicular to the Mo–Mo bond*.

A simple way to contrast the two structures is the following. If we begin with one metal atom and follow the Mo–P, P–C, C–C', C'–C'', C''–P', and P'–Mo' bonds, we may say that all of these bonds are roughly perpendicular to the Mo–Mo' bond except for one C–C bond, which is approximately parallel to the Mo–Mo' bond. In the P molecules, the two parallel C–C bonds are both C–C' (or C'–C'') whereas in the S molecules, one is C–C' and the other is C'–C'' (or vice versa).

**Comparison with Other Molecules.** The majority of  $\beta$ -M<sub>2</sub>X<sub>4</sub>-(diphos)<sub>2</sub> (M = Mo, W) compounds are formed with either diphosphinomethanes or diphosphinoethanes.<sup>11</sup> The former usually have a torsion angle of zero but there are exceptions (e.g., W<sub>2</sub>Cl<sub>4</sub>(dppm)<sub>2</sub> with  $\chi = 17^\circ$ <sup>12</sup>). Compounds with diphosphinoethanes<sup>11</sup> typically show P–M–M–P twist angles of 20–40°. With the larger rings present in the 1,3-dppp compounds, we get larger angles, namely ca. 70° in the P molecules and ca. 75° in the S molecules. This is the first case for a molybdenum compound where we have seven-membered rings, and it is interesting to see that this leads to greater twist angles. In fact, we already have a compound, namely, Mo<sub>2</sub>Cl<sub>4</sub>(*R,R*-DIOP)<sub>2</sub> (DIOP = 2,3-(*O*-isopropylidene-2,3-dihydroxy-1,4-bis(diphenylphosphino)butane) where eight-membered rings are formed, and in that case the P–Mo–Mo–P angles are still larger, namely 78 and 87° for the P and S isomers, respectively.<sup>13</sup>

The closest comparison that can be made with the present compound is the recently reported<sup>14</sup>  $\beta$ -W<sub>2</sub>Cl<sub>4</sub>(dipp)<sub>2</sub>, where dipp

= (Me<sub>2</sub>CH)<sub>2</sub>PCH<sub>2</sub>CH<sub>2</sub>CH<sub>2</sub>P(Me<sub>2</sub>CH)<sub>2</sub>. In its general features, the structure of this compound is very similar to the ones we report here. However, there is *no disorder* in the crystal of the tungsten compound, and only one isomer is present. Remarkably, the isomer present corresponds to the S isomer of the molybdenum compound! This raises the obvious question: Why should the less stable isomer of  $\beta$ -Mo<sub>2</sub>Cl<sub>4</sub>(1,3-dppp)<sub>2</sub> be the *only observed* isomer of  $\beta$ -W<sub>2</sub>Cl<sub>4</sub>(dipp)<sub>2</sub>?

Actually, the inconsistency implied by this question is more apparent than real. In addition, there are other more subtle questions to ask. It must be noted that the ligands in the two cases, one involving Ph<sub>2</sub>P groups and the other (Me<sub>2</sub>CH)<sub>2</sub>P groups, are sufficiently different that both inter- and intramolecular nonbonded forces may be very different in the two cases. Thus, the most stable crystalline phase could well be formed by one isomer in one case and by the other isomer in the other case. The fact that the structure that is dictated by the P isomer of the Mo compound is capable of serving as a host for some S molecules, whereas the crystal formed by one of the isomers of the tungsten compound does not serve as a host for any detectable number of molecules of the second isomer, is not necessarily surprising. Rather small free energy differences are at work in producing such results, and we are not capable of making reliable predictions.

The other, more subtle (and also more interesting) questions that arise are, for example, the following. What will be the ratio of the two isomers in solution? This can probably be answered by NMR studies. NMR data were reported for  $\beta$ -W<sub>2</sub>Cl<sub>4</sub>(dipp)<sub>2</sub> but it is not clear whether they address this question. No NMR data are yet available for  $\beta$ -Mo<sub>2</sub>Cl<sub>4</sub>(1,3-dppp)<sub>2</sub>. We plan to study both cases carefully, in different solvents and at different temperatures. Another question is what effect the introduction of a methyl group on one  $\alpha$ -CH<sub>2</sub> group (thereby giving a chiral center) will have on the conformational preferences and the relative stability of isomers in these systems. Work along this line is already under way, but conclusive results are still lacking owing to problems in obtaining suitable crystals.

**Acknowledgment.** We thank Tong Ren for assistance with the X-ray work and Brian S. Subach for assistance with obtaining crystals. Support from the National Science Foundation at Texas A&M University is gratefully acknowledged. T.J.S. gratefully acknowledges the Research Corp. and the donors of the Petroleum Research Fund, administered by the American Chemical Society, for general support and the National Science Foundation for a Research in Undergraduate Institutions award for the acquisition of the Perkin-Elmer 330 spectrophotometer at Kalamazoo College.

**Supplementary Material Available:** For the crystal structure of  $\beta$ -Mo<sub>2</sub>Cl<sub>4</sub>(1,3-dppp)<sub>2</sub>, tables of bond distances, bond angles, torsion angles, and anisotropic displacement parameters (13 pages); a listing of observed and calculated structure factors (34 pages). Ordering information is given on any current masthead page.

(11) Campbell, F. L.; Cotton, F. A.; Powell, G. L. *Inorg. Chem.* **1985**, *24*, 4384.

(12) Canich, J. A. M.; Cotton, F. A. *Inorg. Chim. Acta* **1988**, *142*, 69.

(13) Chen, J.-D.; Cotton, F. A.; Falvello, L. R. *J. Am. Chem. Soc.* **1990**, *112*, 1076.

(14) Fryzuk, M. D.; Kreiter, C. G.; Sheldrick, W. S. *Chem. Ber.* **1989**, *122*, 851.